IOP Conference Series: Earth and Environmental Science

PAPER • **OPEN ACCESS**

Experimental analysis of the *pseudo-compact* tension (pCT) testing configuration using two alternative sample geometries

To cite this article: M Herbón-Penabad *et al* 2021 *IOP Conf. Ser.: Earth Environ. Sci.* **833** 012033

IOP Conf. Series: Earth and Environmental Science **833** (2021) 012033 doi:10.1088/1755-1315/833/1/012033

Experimental analysis of the *pseudo*-compact tension (*p*CT) testing configuration using two alternative sample geometries

M Herbón-Penabad, A Muñoz-Ibáñez and J Delgado-Martín

School of Civil Engineering, University of A Coruña, Campus de Elviña s/n, A Coruña, 15071, Spain

miguel.herbon@udc.es

Abstract. The pseudo-compact tension (*p*CT) method recently proposed by Muñoz-Ibáñez et al. (2020) is a satisfactory approach to measure mode I fracture toughness (K_{IC}) in rocks and other materials using disc-shaped samples loaded under pure tensile conditions. In contrast to other methods, such as the semi-circular bend (SCB) suggested by the ISRM (2014), the *p*CT test provides with good control after peak load, making it possible to further characterize the processes involved in fracture propagation. In this work we assess the influence of the testing configuration at the onset of unstable crack propagation. In order to extend the *p*CT concept to complementary geometries with potential interest we studied an alternative to the SCB specimen, which we call *pseudo*-SCB (*p*SCB). To compute K_{IC} in this configuration we have derived the corresponding dimensionless stress intensity factor function (Y') based on the finite element method. The results show that the *p*SCB test provides with consistent values of K_{IC} and it also allows to control the propagation of the crack beyond peak load, which reinforces the idea that the loading conditions may be a more determinant factor than the sample geometry in controlling post-peak behaviour. In addition, an expression of Y' is presented for cubic samples tested using the *p*CT approach. This configuration may be useful for testing other materials amenable of moulding such as mortar, concrete, ceramics, etc.

1. Introduction

Mode I fracture toughness (K_{IC}) measures the resistance of a material containing a pre-existing defect to the propagation of tensile cracks [1]. Since rocks are discontinuous at all scales, K_{IC} is of great importance in geotechnical engineering (i.e., tunneling, mining), energy resources exploitation (i.e. geothermal energy, hydraulic fracturing) projects [2-4], etc. In the last years, a number of methods have been proposed to assess K_{IC} in rocks. Worth mentioning among them are the suggested methods endorsed by the International Society for Rock Mechanics (ISRM) [5-7]. The semi-circular bend (SCB) test has favorable features such as simple specimen geometry and testing procedure. However, in this configuration tensile loads are indirectly generated *via* sample compression. In addition, the dynamic unstable fracture propagation prevents post-peak assessment. These drawbacks can be overcome using an alternative testing approach namely pseudo-compact tension (*p*CT), which allow determining K_{IC} under pure tensile conditions with satisfactory control on fracture development after failure [8]. The better performance of the *p*CT method would not be associated to better electronic control or higher stiffness of the testing device but to a lower level of elastic energy storage in the sample during its loading [9]. To check this conjecture, in this study we assess the influence of the loading conditions and specimen geometry on unstable crack propagation. To extend the *p*CT concept to complementary

geometries with potential interest we have studied an alternative to the SCB specimen which we refer as *pseudo*-SCB (*p*SCB). Finally, we extend the compact tension approach to cubic geometries (cubic-*p*CT), which may have a significant interest in materials that, for instance, can be molded such as mortars.

2. Calculation of stress intensity factors

2.1. Specimen geometries

The *p*SCB specimen is based on the SCB sample geometry [7] although incorporating the geometrical features used in the *p*CT configuration to transmit a pure tensile load [8]. As seen in figure 1, *p*SCB samples are semi-circular discs with a centred straight crack starter notch and a U-shaped groove for sample loading. Similar features (groove and straight notch) apply to configuration of cubic-*p*CT specimens. For the two proposed sample geometries, the dimensions of the groove are chosen based on the values suggested for 50 mm-diameter *p*CT specimens [8]. However, a range of notch length ratios (*a/b*) have been considered in the study to investigate the impact in the results. Detailed dimensions of the *p*SCB and cubic-*p*CT specimens are given in table 1.

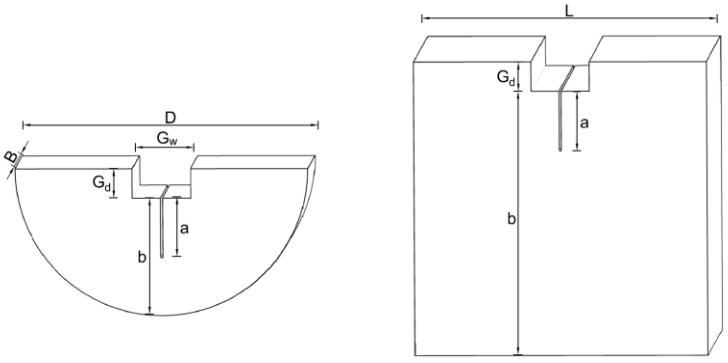

Figure 1. Schematic illustration of the geometry of the pSCB (left) and cubic-pCT (right) specimens. D = diameter; B = thickness; L = side length; G_d = U-shaped groove depth; G_w = U-shaped groove width; a/b = notch length ratio.

Table 1. *p*SCB and cubic-*p*CT specimen dimensions.

Testing method	*D* (mm)	*B/D*	*L* (mm)	G_d (mm)	G_w (mm)	*a/b*
*p*SCB	50 or 54	0.5	-	5	10	0.50-0.75
cubic-*p*CT	-	-	50	5	10	0.20-0.40

2.2. Finite element analysis

The general expression of mode I fracture toughness (K_{IC}) is given in Equation (1), where a is the notch length, σ_{max} is the maximum applied stress, and Y' is the dimensionless stress intensity factor.

$$K_{IC} = Y'\sigma_{max}\sqrt{\pi a} \quad (1)$$

Y' depends not only on the specimen geometry but also on the loading conditions. Several authors have proposed a number of analytical solutions of Y' [10, 11]. However, no closed-form expression could be found in the literature for the two configurations proposed in this work (*p*SCB and cubic-*p*CT), and Y'

was derived for each case using numerical methods. Following the procedure described in [8], Abaqus/Standard version 6.14 was used to compute the mode I stress intensity factor (K_I) using the J-integral method around the notch tip [12]. For the *p*SCB geometry, we modelled specimens of 38, 50 and 100 mm-diameter while for the cubic-*p*CT geometry, only specimens of 50 mm-edge are considered. As reported in previous works [8, 13], the variation in the mechanical properties of the material has a slight effect on K_I, but these differences were found to be irrelevant for computing *Y'*. Therefore, we modelled the material as linear-elastic and isotropic, assuming a Young's modulus of 35 MPa and a Poisson's ratio of 0.3. 2D models of the samples (figure 2) are meshed with 8-node plane strain elements and, in the region defining the crack front, the geometry of the elements is transformed into triangles to consider the stress singularity that occurs at the notch tip [14, 15]. Once a K_I value is obtained from the finite element analysis, *Y'* was derived for each case as follows:

$$Y' = \frac{K_I}{\sigma_0\sqrt{\pi a}} \tag{2}$$

Where σ_0 is the nominal stress acting over the ligament plane for an applied unitary load ($\sigma_0 = P/bB$ or $\sigma_0 = P/bL$, for the *p*SCB and cubic-*p*CT specimens, respectively). The *Y'* results derived were plotted as a function of the notch length ratio (*a/b*) and, by fitting the results with the fourth-order polynomial given in (3):

$$Y' = C_0 + C_1\left(\frac{a}{b}\right) + C_2\left(\frac{a}{b}\right)^2 + C_3\left(\frac{a}{b}\right)^3 + +C_4\left(\frac{a}{b}\right)^4 \tag{3}$$

The coefficients C_i (i = 0-4) are provided in table 2 for each testing configuration and specimen size.

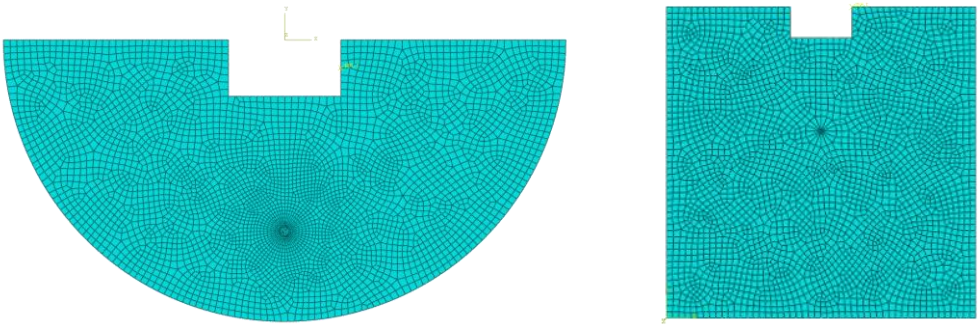

Figure 2. Finite element meshes used for the pSCB (left) and cubic-pCT (right) 2D models.

Table 2. Coefficients (C_i) of the dimensionless stress intensity factor (*Y'*) expression (Eq. 1) derived for the *p*SCB and cubic-*p*CT specimens.

Testing method	*D or L* (mm)	C_0	C_1	C_2	C_3	C_4
*p*SCB	38	189.091	-1275.852	3350.314	-3935.725	1786.012
*p*SCB	50	262.143	-1737.803	4444.301	-5075.795	2226.644
*p*SCB	100	175.378	-1205.393	3235.529	-3867.567	1781.153
cubic-*p*CT	50	6.095	30.193	-200.200	490.880	-381.560

3. Experimental program

3.1. Materials

Three different rock types (two sandstones and one granite) have been used to assess the performance of the *p*SCB test. Reference values for the properties of these materials can be found in [8], and only a short summary is given in Table 3. In the case of cubic-*p*CT tests, experiments were carried out using two generic types of mortar available in the laboratory (HL and HT). In this study, the purpose of K_{IC} testing of mortar samples was limited to demonstration of the performance of the testing method and no additional details on the results and their significance are given.

Table 3. Rock properties: σ_t = indirect tensile strength; K_{IC}^{pCT} = mode I fracture toughness derived with the *p*CT testing method; and K_{IC}^{SCB} = mode I fracture toughness derived with the SCB testing method. Data for Corvio sandstone corresponds to 50- mm in diameter specimens.

Rock type	σ_t (MPa)	K_{IC}^{pCT} (MPa m$^{1/2}$)	K_{IC}^{SCB} (MPa m$^{1/2}$)
Corvio sandstone	1.9-3.1	0.07-0.12	0.12-0.18
Pinacas sandstone	11.2-11.8	1.33 ± 0.03	1.27 ± 0.05
Blanco Mera granite	9.7	1.21 ± 0.03	1.25 ± 0.04

3.2. Sample preparation

The *p*SCB samples were obtained from rock cores of 50 and 54 mm-diameter. The cores were first sliced into discs, and then diametrically halved using a customized tile saw (figure 3). The U-shape groove and the straight notch were cut subsequently following the procedure described in [8] for *p*CT specimens. Specially-designed 3D-printed fixtures were used to hold the samples in place during machining (figure 3). For the cubic-*p*CT specimens (50 mm-edge), once demoulded they were processed using the same approach to cut the groove and notch.

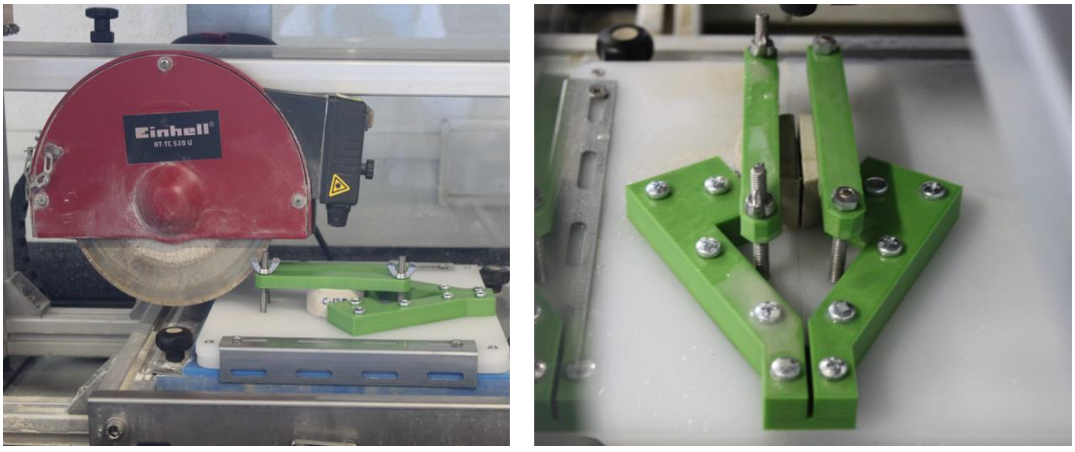

Figure 3. Customized tile saw used to prepare the samples (left) and detail of the 3D printed fixtures used to hold the rock discs when they are diametrically-halved (right).

3.3. Mode I fracture toughness tests

*p*SCB and cubic-*p*CT samples were tested using a loading frame equipped with a 50 kN load cell already presented in [8]. To carry out the tests, the samples are placed on a small removable cradle (figure 4)

which is rose to fit the U-groove between the couple of hardened steel jaws, one of them programmed to move at a constant rate to provide the tensile load to the specimen. At a certain loading level, the stress concentration at the notch tip generates a crack that propagates along the ligament plane.

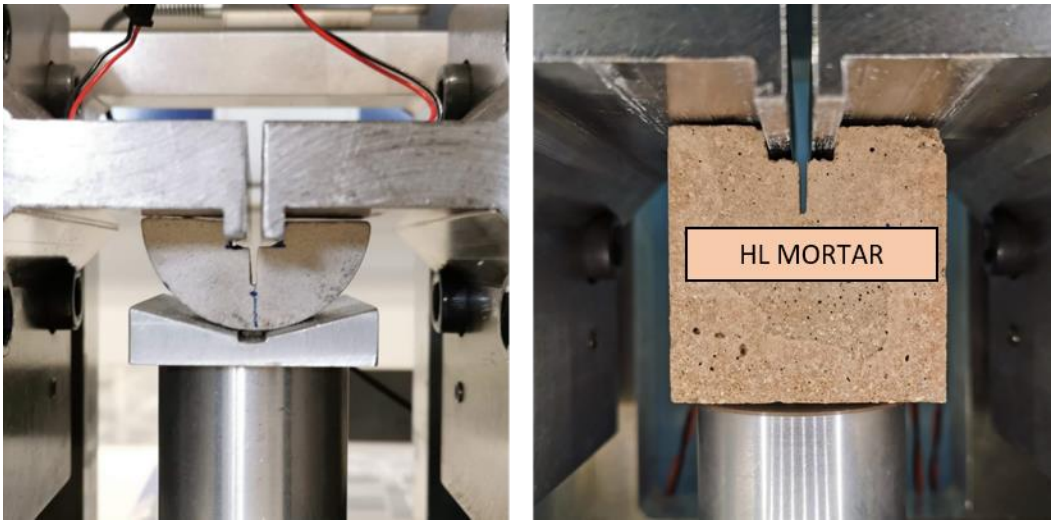

Figure 4. Experimental setups for pSCB (left) and cubic-pCT tests (right).

All the tests were carried out at room temperature conditions and at a loading rate of 0.1 mm/min, following the recommendations given to conduct *p*CT experiments [8]. Load (P) and load point displacement (LPD) were continuously recorded during the tests. LPD corresponds to the displacement of the right steel jaw and it is measured through two linear variable differential transducers (LVDT) placed symmetrically on both sides of the specimen. Mode I fracture toughness (K_{IC}) was derived using Equation (4):

$$K_{IC} = Y' \frac{P_{max}}{bB} \sqrt{\pi a} \tag{4}$$

where Y' is the dimensionless stress intensity factor computed from Equation (1), P_{max} is the peak load, b is the distance from the base of the groove to the bottom of the specimen, B is the specimen thickness, and a is the notch length. For 54 mm-diameter *p*SCB specimens, Y' was computed interpolating the coefficients given in table 2 for 50 and 100 mm-diameter specimens.

4. Results and discussion

4.1. Loading curves

Figure 5 shows typical P *vs.* LPD curves for the samples tested in this study. For the two testing methods and materials considered, we observe that it is possible to identify the three main stages described in [8]: a first period of linear elastic increase, a non-linear stage close to P_{max}, and a post-peak branch. In the pre-peak region, the slope of the curve and the extent of the non-linear domain are highly dependent on the material being tested. This has been already discussed in [9]. It is interesting to note that all the experiments performed in this study could be conducted beyond P_{max} in a controlled manner. That suggests that the post-peak control does not depend on the geometry of the tested specimen but from a combination of how loads are delivered, rate of loading and eventually the intrinsic properties of the tested material. Considering the poorer performance of the conventional SCB test (which takes place

under bending conditions) the cross comparison of results using the same materials [9] make us conclude that loading under pure tension is critical for a good control of the post-peak behaviour and the investigation of fracture propagation.

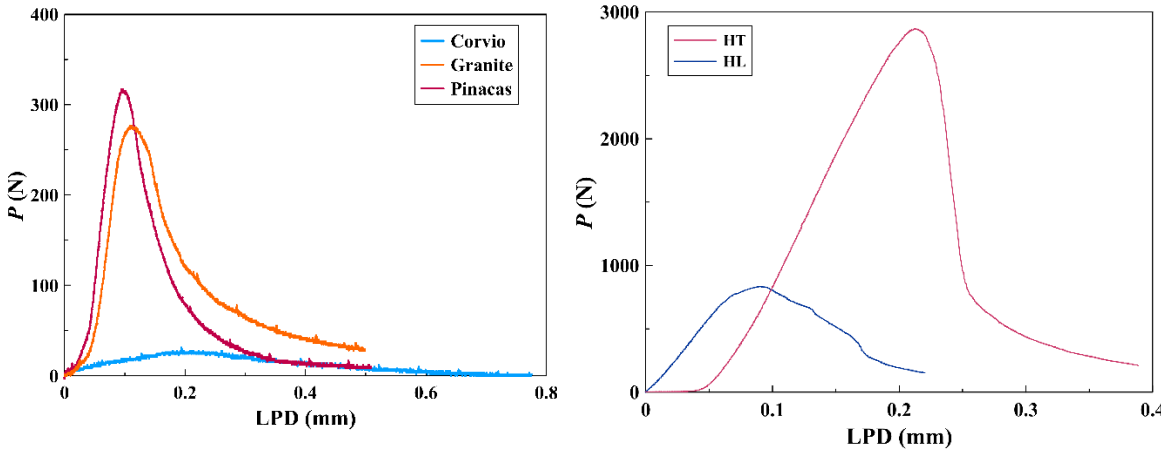

Figure 5. P vs. LPD curves for pSCB tests performed with rock samples (left), and cubic-pCT tests performed with mortar samples (right).

4.2. Mode I fracture toughness of rock samples

Mode I fracture toughness (K_{IC}) have been computed at the level I testing using the values of peak load recorded from the experiments. To assess repeatability of results, we performed a statistical analysis for each material using the free software Past 3.0 [16]. K_{IC} values conform to normal distributions considering a significance level of 95% for the three lithologies and two types of mortar tested. Mean values of K_{IC} derived from the *p*SCB and cubic-*p*CT experiments are listed in table 4.

Table 4. Mode I fracture toughness (K_{IC}) derived with the *p*SCB and cubic-*p*CT testing method (mean ± standard error of the mean). Number of tests (into brackets) and specimen size (D = diameter; L = side length) are also given.

Material	D *or* L (mm)	K_{IC}^{pSCB} (MPa m$^{1/2}$)	$K_{IC}^{cubic\text{-}pCT}$ (MPa m$^{1/2}$)
Corvio sandstone	50	0.16 ± 0.01 (7)	-
Pinacas sandstone	50	0.95 ± 0.03 (3)	-
Blanco Mera granite	54	0.83 ± 0.08 (5)	-
HL	50	-	0.40 ± 0.01 (5)
HT	50	-	1.16 ± 0.02 (5)

K_{IC} values derived for Corvio sandstone obtained via the *p*SCB method are in good agreement with those reported in table 2 for SCB tests [9]. Curiously, these values even conform to a normal distribution, which contrasts with the behavior observed for *p*CT and SCB samples of same size (D = 50 mm) in [9]. This suggest that, for this rock type, the *p*SCB configuration has the potential to provide with better repeatability compared with than other testing approaches. However, further tests are required to confirm this perception. On the other hand, it should be noted that the values of K_{IC} obtained for Pinacas

sandstone and Blanco Mera granite are comparatively lower (~30%) than those delivered for the *p*CT and SCB tests using 50-mm in diameter samples. In fact, the K_{IC} results reported in this study are within the range of those observed for smaller (D = 38 mm) SCB samples (K_{IC} ~ 0.7-1.1 MPa $m^{1/2}$ for Pinacas sandstone, and K_{IC} ~ 0.7-0.9 MPa $m^{1/2}$ for Blanco Mera granite). We conjecture that the length of the ligament may be a determinant factor in fracture toughness determination, and that a minimum length would be needed to provide consistent K_{IC}.

5. Conclusions

Two alternative sample geometries (*p*SCB and cubic-*p*CT) for measuring mode I fracture toughness using the pseudo-compact tension (*p*CT) loading configuration are presented and described. Expressions of the dimensionless stress intensity factors (Y') were derived for each testing configuration using numerical models. The pseudo-semicircular bend (*p*SCB) specimen, which is based on the SCB geometry proposed by the ISRM, was used to assess the K_{IC} of three different lithologies: Corvio and Pinacas sandstones, and Blanco Mera granite. The K_{IC} values obtained conform to normal distributions irrespective of rock type. That suggests that the *p*SCB test could provide with satisfactory repeatability of K_{IC} measurements. However, it should be noted that the number of tests reported in this study may be limited to come to a firm conclusion. Further testing would be necessary in this regard. In addition, some results of K_{IC} obtained in this study for the *p*SCB approach are comparatively lower than those reported previously for the same rock types and specimen sizes using different testing methods. We conjecture that this behavior could be related to the shorter ligament length of the *p*SCB specimens, which would imply that larger specimens would be needed to deliver a consistent value of fracture toughness using this approach. Finally, it was proved that the *p*CT configuration provides with a satisfactory control on the post-peak region (i.e., unstable fracture propagation) with independence on the sample geometry (i.e. circular, semicircular, or cubic), suggesting that this configuration could be an interesting approach for measuring K_{IC} not only in rocks but also in other geomaterials.

Acknowledgements

This work was funded by the MINECO/AEI/FEDER, UE project BIA2017- 87066-R

References

[1] Whittaker BN, Singh RN and Sun G 1992 *Rock fracture mechanics: principles, design, and applications* (Amsterdam: Elsevier)

[2] Nasseri MHB, Schubnel A and Young RP 2007 Coupled evolutions of fracture toughness and elastic wave velocities at high crack density in thermally treated Westerly granite *Int J Rock Mech Min Sci* **44** 601–16

[3] Major JR, Eichhubl P, Dewers TA and Urquhart AS 2014 The effect of CO_2-related diagenesis on geomechanical failure parameters; fracture testing of CO_2-altered reservoir and seal rocks from a natural analog at Crystal Geyser *48th US Rocks Mech Symp, Utah, USA* 14–7463:1–5

[4] Talukdar M, Guha Roy D and Singh TN 2018 Correlating mode-I fracture toughness and mechanical properties of heat-treated crystalline rocks *J Rock Mech Geotech Eng* **10** 91–101

[5] ISRM 1978 Suggested methods for determining tensile strength of rock materials *Int J Rock Mech Min Sci Geomech Abstr* **15** 99–103

[6] ISRM 1988 Suggested methods for determining the fracture toughness of rock *Int J Rock Mech Min Sci Geomech Abstr* **25** 71–96

[7] Kuruppu MD, Obara Y, Ayatollahi MR, Chong KP and Funatsu T 2014 ISRM-suggested method for determining the mode I static fracture toughness using semi-circular bend specimen *Rock Mech Rock Eng* **47** 267–74

[8] Muñoz-Ibáñez A, Delgado-Martín J, Costas M, Rabuñal-Dopico J, Alvarellos-Iglesias J and Canal-Vila J 2020 Mode I fracture toughness determination in rocks using a pseudo-compact

tension (*p*CT) test approach *Rock Mech Rock Eng g* **53** 3267-85
[9] Muñoz-Ibáñez A, Delgado-Martín J and Juncosa-Rivera R 2021 Size effect and other effects on mode I fracture toughness using two testing methods *Int J Rock Mech Min Sci* **143C** 104785
[10] Liu A 1996 Summary of Stress-Intensiy Factors *ASM Handbook. Fatigue and Fracture* vol 19 ed ASM International pp 980-1000
[11] Fett T and Munz D 1997 *Stress intensity factors and weigth functions* (Southampton: Computational Mechanics Publications)
[12] Qian G, González-Albuixech VF, Niffenegger M and Giner E 2016 Comparison of K_I calculation methods *Eng Fract Mech* **156** 52–67
[13] Tutluoglu L and Keles C 2011 Mode I fracture toughness determination with straigth notched disk bending method *Int J Rock Mech Min Sci* **48** 1248-61
[14] ABAQUS 2014 *ABAQUS Version 6.14/analysis user's guide* Dassault Systemes Simulia Corporation, Providence, Rhode Island.
[15] Ayatollahi MR, Mahdavi E, Alborzi MJ and Obara Y 2016 Stress intensity factors of semi-circular bend specimens with straightthrough and chevron notches *Rock Mech Rock Eng* **49** 1161–72.
[16] Hammer Ø 2011 PAST PAleontological STatics Reference Manual. *Natural Hist Museum*. 201248